Annals of Glaciology 33 2001

Snow-ice accretion and snow-cover depletion on Antarctic first-year sea-ice floes

Martin O. Jeffries,[1] H. Roy Krouse,[2] Barbara Hurst-Cushing,[1] Ted Maksym[1]
[1]*Geophysical Institute, University of Alaska Fairbanks, Fairbanks, AK 99775-7320, U.S.A.*
[2]*Department of Physics and Astronomy, University of Calgary, 2500 University Drive N.W., Calgary, Alberta T2N 1N4, Canada*

ABSTRACT. Between austral late winter 1993 and austral autumn 1998, during five cruises aboard the research vessel *Nathaniel B. Palmer*, almost 300 m of core was obtained from first-year ice floes in the Ross, Amundsen and Bellingshausen Seas. Analysis of the texture, stratigraphy and stable-isotopic composition of the ice was used to assess the magnitude of the role of flooding and snow-ice formation at the base of the snowpack in the thickening of the ice cover and the thinning of the snow cover. Snow ice occurred in all ice-thickness categories and made a significant contribution to the total ice mass (12–36%) in both autumn and winter. Although the amount of snow ice was often exceeded by the amount of frazil ice and congelation ice, the thickness of individual layers of each ice type indicated that snow ice often made a greater contribution to the thermodynamic thickening of the ice cover than the other ice types. The larger quantities of frazil ice and congelation ice were primarily the result of dynamic thickening. Flooding and snow-ice formation reduced the snow cover to 42–70% of the total snow accumulation depending on time and location. On the basis of this information, ship-based snow-depth estimates were adjusted to estimate the total snow accumulation on different ice-thickness categories.

INTRODUCTION

Snow-covered sea ice is an effective barrier that has a significant impact on the exchange of heat, mass and momentum between the ocean and the atmosphere, thereby influencing climate from local to global scales (Allison, 1982). In Antarctica, recognition of this fact led to increased efforts in the latter part of the 20th century to document the depth of the snow cover, the thickness of the ice and the processes by which the ice thickens. As a consequence, it is now apparent that over broad areas of the pack ice the floes thicken as a result of flooding and snow-ice formation at the base of the snowpack (Lange and others, 1990; Allison and Worby, 1994; Eicken and others, 1994, 1995; Jeffries and others, 1994a, 1997, 1998; Jeffries and Adolphs, 1997; Massom and others, 1997, 1998; Adolphs, 1998; Rapley and Lytle, 1998; Maksym and Jeffries, 2000).

Flooding occurs at the base of the snowpack when the snow load is sufficient to overcome the buoyancy of the ice, and seawater and brine exchange occurs between the ocean and the top of the ice. Subsequent freezing of the mixture of snow (meteoric ice) and sea water/brine leads to the formation of snow ice that becomes an integral part of the floe. Flooding and snow-ice formation are key processes that affect the energy and mass budget, biological productivity, electromagnetic properties and remote sensing of the Antarctic sea ice and its snow cover, and set it apart from Arctic sea ice and its snow cover (Fritsen and others, 1994, 1998; Lytle and Ackley, 1996; Lytle and others, 1996; Drinkwater and Lytle, 1997; Morris and others, 1998; Sturm and others, 1998).

Most reports of snow-ice occurrence have been based on ice-core data obtained during a single cruise. This limits the understanding of the spatial and temporal variability of snow-ice formation and its role in the thickening of the ice cover. Since 1993 we have investigated snow-ice occurrence during five autumn and winter cruises in the Ross, Amundsen and Bellingshausen Seas, Antarctica. During those five cruises, a program of standardized snow and ice observations (Worby and Allison, 1999), including snow-depth estimates, was maintained while the ship was underway in the pack ice. The snow and ice observations are contributed to the Scientific Committee on Antarctic Research (SCAR) sponsored Antarctic Sea-Ice Processes and Climate (ASPeCt) program, which aims to obtain data for the forcing and validation of numerical simulations of sea-ice processes and atmosphere–ice–ocean interactions (Worby and Ackley, 2000). However, as a result of snow-ice formation and the entrainment of snow into the underlying ice floes, the snow cover must be depleted and snow-depth estimates do not represent the total snow accumulation. This has important implications for the representativeness of ship-based snow-depth estimates and their use for model forcing and validation.

The primary purpose of this paper is to provide a comprehensive overview of the temporal and spatial variability of snow-ice occurrence and its contribution to the thermodynamic thickening and mass budget of ice cover relative to frazil and congelation ice in this Pacific sector of the Southern Ocean. The secondary purpose is to determine the proportion of the total snow accumulation that remains on the floes after snow-ice formation, and to adjust ship-based snow-depth estimates to derive improved estimates of total snow accumulation on different ice-thickness categories.

STUDY AREA

The locations of the five cruises aboard the research vessel *Nathaniel B. Palmer* are shown in Figure 1. During the autumn

https://doi.org/10.3189/172756401781818266 Published online by Cambridge University Press

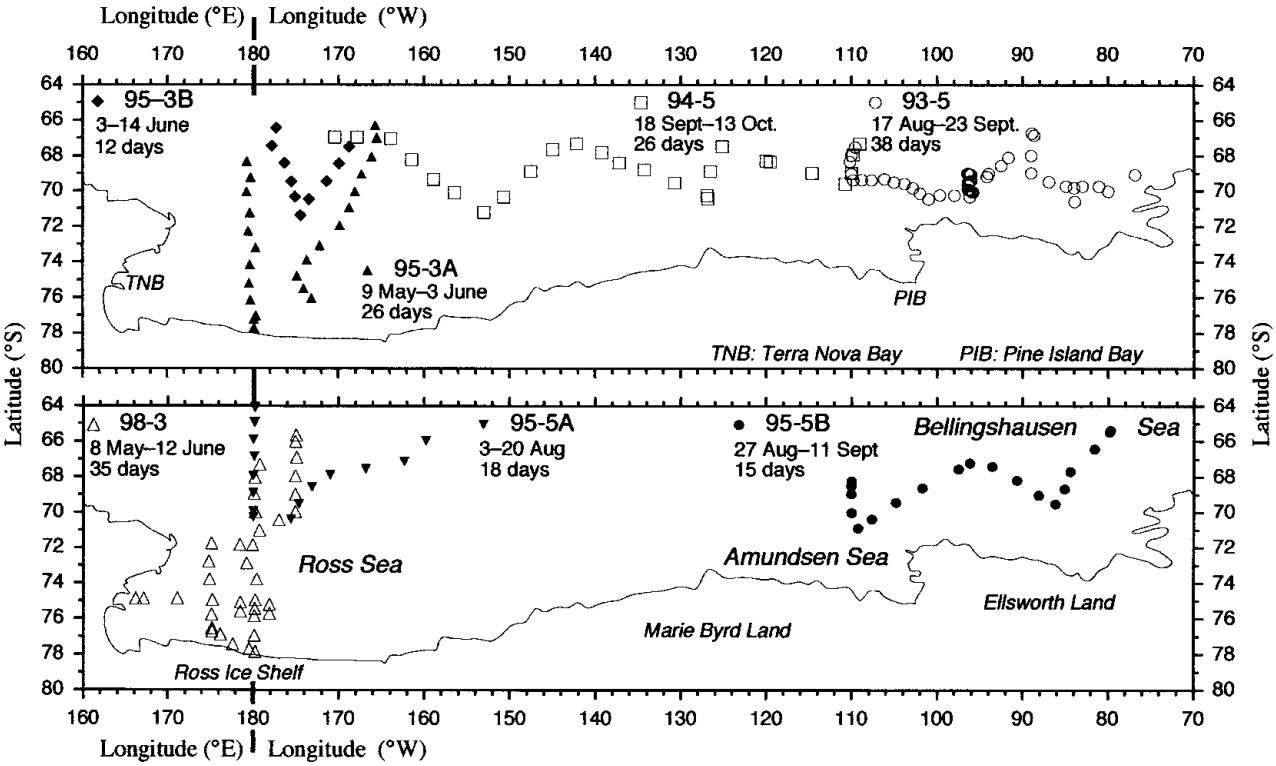

Fig. 1. Maps showing the location, dates and duration of cruises aboard the R/V Nathaniel B. Palmer *in the autumn and winter pack ice of the Ross, Amundsen and Bellingshausen Seas.*

cruises in the Ross Sea (NBP 95-3, 98-3) we succeeded in crossing the entire ice pack between the ice edge and the continent. NBP 95-3 is divided into two basic parts: 95-3A, the initial, long southbound and northbound legs through the entire pack ice, and 95-3B, the later, shorter southbound and northbound legs between the ice edge and the central pack ice. The NBP 95-3B data are kept apart from the 95-3A data in order to minimize any bias likely to accrue due to the large number of stations between the ice edge and the central pack ice. The NBP 95-3A and 98-3 cruises are each further divided into two parts (95-3Ai, 95-3Aii, 98-3i, 98-3ii) on the basis of snow-ice occurrence. During the winter cruises (NBP 93-5, 94-5, 95-5A, 95-5B), thicker ice, deeper snow cover and time constraints impeded progress and prevented the continent from being reached. Nevertheless, Figure 1 shows that, as a result of the five cruises, a large proportion of the Ross, Amundsen and Bellingshausen Seas was covered during May, June, August, September and October, some areas were sampled twice in the same year (NBP 95-3Ai, 95-3B and 95-5A) and other areas were sampled twice but in different years (NBP 93-5 and 95-5B, and NBP 95-3Aii and 98-3ii).

METHODS

Ice cores were obtained at 3–5 points on 100–150 m long transects on floes, except in 1993, when we obtained only a single core from most floes. The cores were obtained from "level" ice, which was invariably rafted but not ridged. On all cruises, single cores were often also obtained from floes that were too small for drilling transects, particularly in the marginal ice zones. Information on the lengths of the cores is summarized in Table 1.

On being removed from the ice, the base of each core was examined to determine whether bottom melting was occurring, as indicated by a smooth, scalloped ice/water interface, or whether bottom freezing was occurring, as indicated by the presence of a soft skeletal layer associated with active

Table 1. Information on number of ice floes sampled, number and length of ice cores, total length of ice core analyzed for texture/stratigraphy, and number of stable- isotope measurements made subsequent to the texture/stratigraphy analysis

Cruise (NBP)	*Number of floes*	*Number of ice cores*	*Min. core length*	*Max. core length*	*Mean core length*	*Total length of core analyzed for texture*	*No. of stable-isotope measurements*
			m	m	m	m	
93-5	50	63	0.14	2.24	0.84	52.08	524
94-5	26	73	0.055	4.39	0.74	61.03	735
95-3A	29	70	0.11	2.10	0.58	40.93	683
95-3B	15	30	0.24	1.03	0.56	16.78	152
95-5A	27	54	0.205	1.28	0.66	35.76	494
95-5B	19	48	0.215	4.06	0.86	41.59	547
98-3	33	91	0.02	1.605	0.54	49.36	688

https://doi.org/10.3189/172756401781818266 Published online by Cambridge University Press

congelation-ice formation. Each core was then taken to the ship and kept frozen until its texture and stratigraphy were determined later in the day in the science freezer at a temperature of −15° to −20°C. After splitting the cores longitudinally using a band-saw, vertical thick (1–2 mm) sections were cut and then illuminated between crossed polarizers to reveal the crystal texture. The textural variability and stratigraphy were recorded, including the thickness of the layers of ice that appeared to be stacked one upon the other, as described by Jeffries and others (1997, 1998).

Each core was then sampled according to the observed layering for later stable-isotope analysis. Depending on core length, and stratigraphic and textural variability, between 4 and 38 contiguous samples were taken per core for stable-isotope analysis. The oxygen isotopic composition of each melted ice sample was determined using standard procedures and the values expressed as δ^{18}O in parts per thousand (‰) relative to the standard V-SMOW (Vienna Standard Mean Ocean Water), as described in Jeffries and others (1994a). The total length of ice core examined during each cruise for stratigraphic/textural/isotopic variability, and the total number of samples analyzed for their $^{18}O/^{16}O$ ratios are summarized in Table 1.

As a complement to the ice-core analysis, the snow cover and sea water were also sampled for stable-isotope analysis. The snow samples were those that had been obtained initially for studies of the physical characteristics of the snow cover (Jeffries and others, 1994b; Sturm and others, 1998; Morris and Jeffries, 2001). Once the investigation of each ice floe had been completed, a water sample was obtained from the uppermost 10–15 m of the ocean mixed layer using standard oceanographic sampling techniques.

The columnar texture of congelation ice that forms as sea water freezes at the base of the ice cover is easily distinguished from granular ice. Granular ice, on the other hand, originates as either frazil ice or snow ice. Consequently, stable-isotope data are required to aid in their identification (Lange and others, 1990). We assumed that any granular ice layer with a δ^{18}O value <0‰ was snow ice, while any granular ice with a δ^{18}O value ≥0‰ was frazil ice. This approach provides a plausible upper limit to the amount of snow ice (Jeffries and others, 1997), and is the same threshold used by investigators in other regions of the Southern Ocean (Lange and others, 1990; Allison and Worby, 1994; Eicken and others, 1994, 1995; Worby and Massom, 1995). Once the granular ice in the original ice-core texture logs had been assigned to either the frazil-ice or snow-ice category, the amount of snow ice, frazil ice and congelation ice in each core and in the set of cores from each cruise was calculated. The amount of each ice type is presented as a proportion of the total length of a set of cores (Jeffries, 1997).

To determine the fraction of snow in the snow ice we used a simple isotopic balance model:

$$f_s + f_{sw} = 1 \quad (1)$$

$$f_s\delta_s + f_{sw}\delta_{sw} = \delta\,, \quad (2)$$

where f_s is the snow fraction, f_{sw} is a sea-water fraction, δ_s is the measured δ^{18}O value for snow, δ_{sw} is the measured sea-water δ^{18}O value, and δ is the measured δ^{18}O value of the snow-ice layer for which the snow fraction is being determined. The snow fraction of the entire core, F_m, is calculated according to:

$$F_m = f_s(h_i/h_c)\,, \quad (3)$$

Table 2. Mean (±1 standard deviation) δ^{18}O values for snow and sea water. The number of measurements is given in parentheses

Cruise (NBP)	Snow δ^{18}O ‰	Sea-water δ^{18}O ‰
93-5	−13.2 ± 3.8 (59)	−0.9 ± 0.4 (36)
94-5	−17.3 ± 3.3 (222)	−0.8 ± 0.1 (23)
95-3	−19.3 ± 4.8 (235)	−1.1 ±0.5 (25)
95-5A	−18.4 ± 4.2 (145)	−1.7 ± 0.4 (15)
95-5B	−15.9 ± 4.1 (102)	−0.9 ± 0.1 (17)
98-3	−19.8 ± 6.6 (132)	−0.6 ± 0.3 (28)

where f_s is the snow fraction of the snow ice in the core, h_i is the thickness of the snow ice and h_c is the length of the core (Jeffries and others, 1994a).

Snow depth was measured at 1 m intervals along the 100–150 m long transects on individual ice floes. Known as Set A (Worby and others, 1996), these data permit a detailed description of small-scale snow-depth variability. While the ship was underway in the ice, 25 estimates of snow depth and ice thickness were made each hour as floes were turned on their side by the ship. Known as Set B (Worby and others, 1996), these data permit a description of the broad spatial variability of snow depth and ice thickness throughout the ice pack. The Set A and B data are used to estimate the proportion of the total snow accumulation that remained after snow has been entrained into floes by snow-ice formation, and to adjust observed snow-depth data to obtain an improved estimate of total snow accumulation.

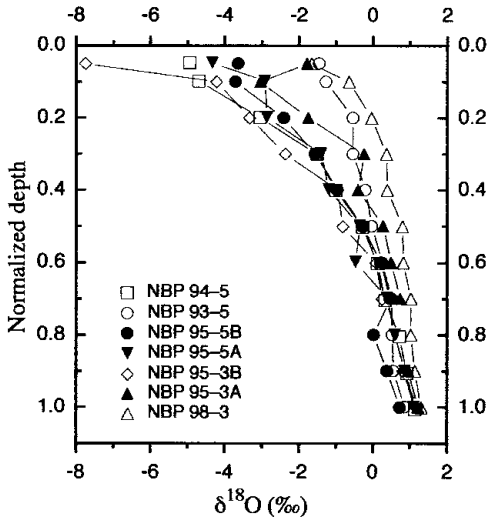

Fig. 2. Composite δ^{18}O profiles representing the average of all the δ^{18}O profiles in all the ice cores obtained during each cruise. Because the ice cores were sampled for stable isotopes at irregular intervals according to their stratigraphy, the following procedure was adopted for compiling the profiles: the depth for each δ^{18}O value was normalized by dividing by the ice-core length; the δ^{18}O values were binned between the surface and the base of the ice at 11 normalized depth intervals of 0.05, 0.1, 0.2 and so on at intervals of 0.1; and a mean δ^{18}O was calculated for each bin. Each data point in a profile represents the mean δ^{18}O value for each bin.

https://doi.org/10.3189/172756401781818266 Published online by Cambridge University Press

Table 3. Number of ice cores containing snow ice, frazil ice and congelation ice (figures in parentheses represent the proportion of the total number of cores)

Cruise (NBP)	Number of cores with snow ice	Number of cores with frazil ice	Number of cores with congelation ice
93-5	51 (81%)	57 (90%)	45 (71%)
94-5	69 (95%)	46 (96%)	43 (90%)
95-3A	59 (84%)	53 (75%)	64 (91%)
95-3B	26 (86%)	25 (83%)	26 (86%)
95-5A	49 (91%)	39 (72%)	46 (85%)
95-5B	44 (92%)	55 (75%)	66 (90%)
98-3	65 (71%)	85 (93%)	75 (82%)

RESULTS AND DISCUSSION

Ice-core δ^{18}O profiles, snow-ice occurrence and snow fractions

The snow ice is differentiated from frazil ice on the basis of differences in their isotopic composition, which arise because frazil ice originates from sea water, while snow ice originates from a mixture of sea water and snow. This concept is illustrated by the δ^{18}O values for snow and sea water (Table 2) and the composite ice-core δ^{18}O profiles (Fig. 2) for each cruise. The δ^{18}O profiles share two basic features. First, the values at the bottom of the ice are all similar and about 2‰ more positive than the sea-water values (Table 2) due to isotopic fractionation during freezing, which enriches the ice in the heavy isotope. Second, the δ^{18}O values in the uppermost ice layers are all more negative than those in the lower ice layers and the sea water. This reflects the entrainment of snow into the floes as the base of the snow is flooded with sea water and snow/sea-water mixture subsequently freezes to form snow ice. The δ^{18}O values of snow ice are intermediate between those of snow and sea water and depend on the fraction of each component, and the extent of isotopic fractionation that occurred as the snow/sea-water mixture froze and snow ice formed.

The δ^{18}O profiles indicate that there was a significant amount of snow ice in the cores. A majority of cores examined during each cruise did indeed contain snow ice (Table 3) and it occurred in all thickness categories (Fig. 3). The bulk of the snow ice occurred on ice of intermediate (0.3–1.2 m) thickness. Occasionally, a relatively large amount of snow ice also occurred on thin (<0.3 m) and thick (>1.2 m) ice. This suggests that sufficient snow can accumulate quickly on young ice to overcome the buoyancy of the ice, leading to flooding and snow-ice formation. Sufficient snow can also accumulate on the thickest ice to overcome its buoyancy. Regardless of the differences between ice-thickness categories, and the spatial and temporal variability evident from cruise to cruise, the essential aspect of the snow-ice data is that, regardless of time, location and ice thickness, snow ice was ubiquitous and had made a substantial contribution to the thickening of much of the ice cover prior to sampling. A total length of 297 m of ice core had been examined after five cruises: 24.5% of that ice was snow ice (Fig. 3d).

To solve for f_s, the fraction of snow in the snow ice, required δ^{18}O values for sea water (δ_{sw}), snow (δ_s) and the snow ice (δ). The δ values are those of the snow-ice sample for which f_s is being determined. For δ_{sw} we had to use a δ^{18}O value of 0‰ rather than the values in Table 2, since we assume that all granular ice with a value <0‰ was snow ice (Jeffries and others, 1997). For δ_s for each cruise we used the mean and standard deviation values shown in Table 2 (e.g. for cruise NBP 93-5 we used values of −9.4‰, −13.2‰ and −17.0‰, i.e. −13.2 ± 3.8‰, to calculate f_s values). Using a range of δ_s values allows for the variability of snow δ^{18}O values that is likely to arise due to atmospheric processes that affect the isotopic ratio of the

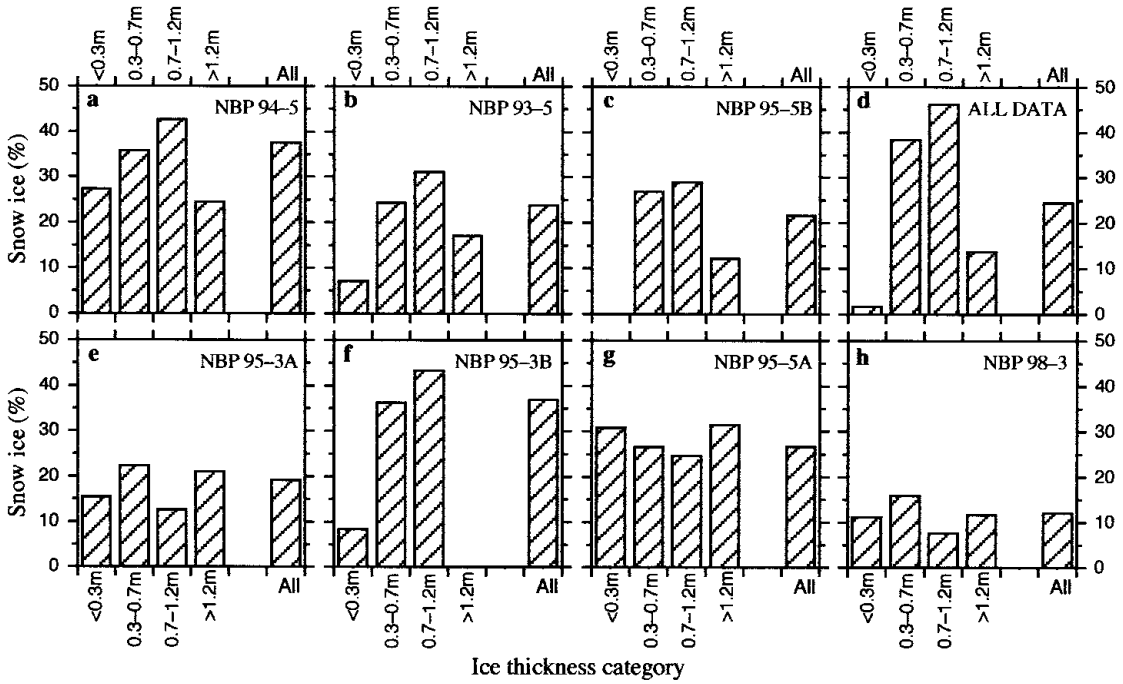

Fig. 3. (a–h) Amounts of snow ice as a proportion of the total length of core examined in four ice-thickness categories and in all those categories combined during each cruise. The amount of snow ice in each thickness category as a proportion of the total length of core examined during all the cruises is shown in (d). The ice-thickness categories are based on the WMO Sea Ice Nomenclature (WMO, 1970) used in standardized ship-based observation and characterization of the Antarctic pack ice (Worby and Allison, 1999).

https://doi.org/10.3189/172756401781818266 Published online by Cambridge University Press

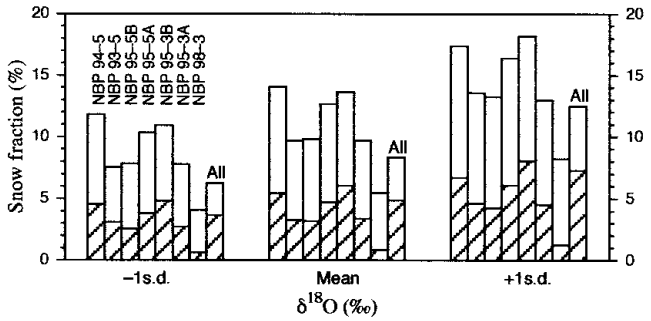

Fig. 4. Bar graphs showing the mean snow fraction of the snow-ice layers (f_s) and the mean snow fraction of the entire ice thickness (F_m) during each cruise. The short, cross-hatched bars represent F_m. f_s is represented by the height of the open bars plus the cross-hatched bars below.

moisture prior to and during precipitation events, and from factors such as metamorphism, wind erosion and redeposition that affect the isotopic composition of the snow cover once it has been deposited on the floes.

The mean f_s and F_m values calculated using three different δ_s values for individual cruises are illustrated in Figure 4. Depending on δ_s, f_s varied between 4% and 18%, while F_m varied between 0.6% and 8%. The lowest f_s and F_m values occurred in the NBP 98-3 cores. Why those f_s values were so low is unclear, but the low F_m values can be attributed with certainty to the fact that the snow-ice layers were particularly thin for this cruise, as will be shown later. Combining all the cruise data gives mean f_s values of 6.25–12.5% and mean F_m values of 3.65–7.3% (Fig. 4: All). Whether one considers the snow fractions for individual cruises or for all the cruises combined, the f_s and F_m values are similar to those reported in the Weddell Sea (Lange and others, 1990; Eicken and others, 1994, 1995). All published f_s and F_m values are probably conservative estimates because some of the snow entrained in the sea water during flooding dissolves in the melt and is subsequently transferred out of the incipient snow-ice layer as it freezes and some of the rejected brine flows into the underlying ice (Maksym and Jeffries, 2001).

Though the f_s and F_m values may be conservative, it is apparent from the snow fraction data that the snow entrained in floes as a consequence of snow-ice formation was a modest proportion of the total ice mass in the Ross, Amundsen and Bellingshausen Seas. However, the snow ice itself comprised a more significant proportion of the ice mass (Fig. 3). Just how significant snow-ice formation was to the thickening and mass budget of the ice cover relative to the other two main ice types, frazil and congelation ice, is discussed in the next subsection.

Snow ice, frazil ice and congelation ice: temporal and spatial variability and their role in the thermodynamic thickening of the ice cover

A majority of ice cores on each cruise also contained frazil ice and congelation ice (Table 3). Snow ice, frazil ice and congelation ice commonly occurred together in most cores, but there was considerable spatial and temporal variability in terms of their contribution to the total ice mass (Fig. 5). This variability can be condensed into three main points:

1. ice composition in late winter in the eastern region (80–110° W; NBP 93-5, 95-5B) was almost identical in two different years, and the eastern and central (110–170° W;

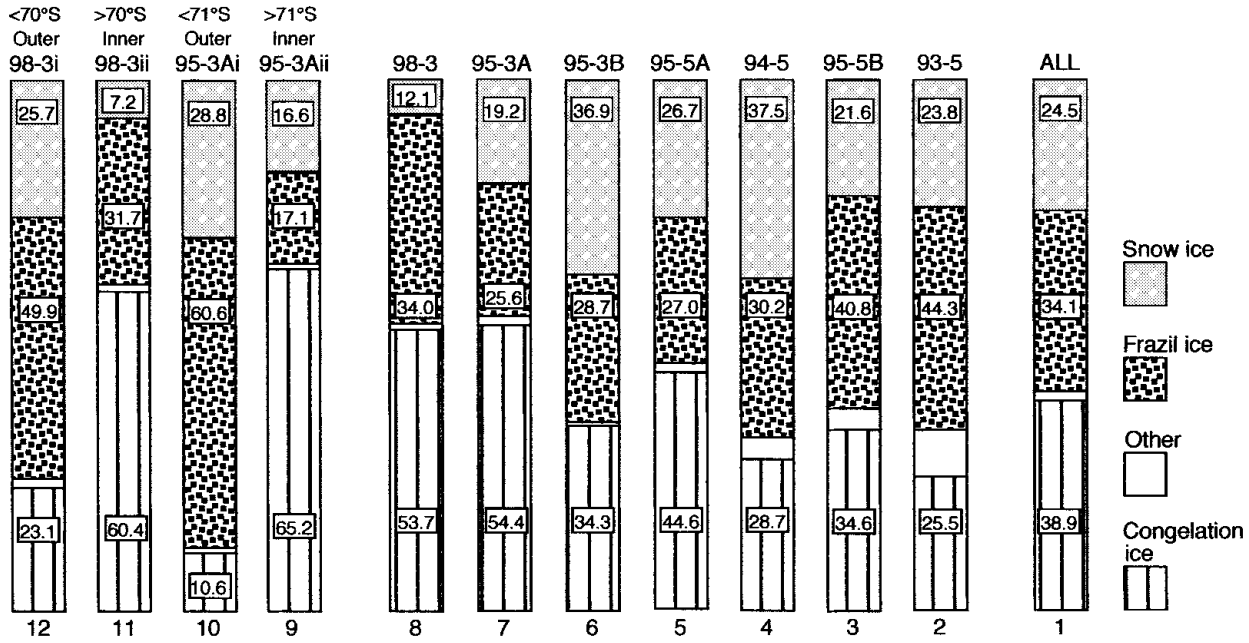

Fig. 5. Proportional representation of the amounts of snow ice, frazil ice, congelation ice and other ice observed in ice cores. Each column represents the total length of ice core normalized to 1 or 100%. The proportion of each ice type is represented by the length of the space it occupies within the column and by the value in each space. Column 1 represents the total length of core analyzed on all the cruises combined. Columns 2–8 represent the total length of core analyzed on each cruise and they are arranged in sequence from right to left, east to west, to show the variability in the study area. Columns 9–12 represent the total length of core analyzed in the outer and inner pack ice of the Ross Sea in May/June 1995 and 1998. Other ice includes fragmented ice and cavities; the latter are slush- or water-filled gaps between ice blocks sometimes encountered in floes where the ice has not consolidated completely since being deformed. Cavities are identified as an ice type because they are a part of the total ice thickness and represent the consequences of a particular mode of thickening.

https://doi.org/10.3189/172756401781818266 Published online by Cambridge University Press

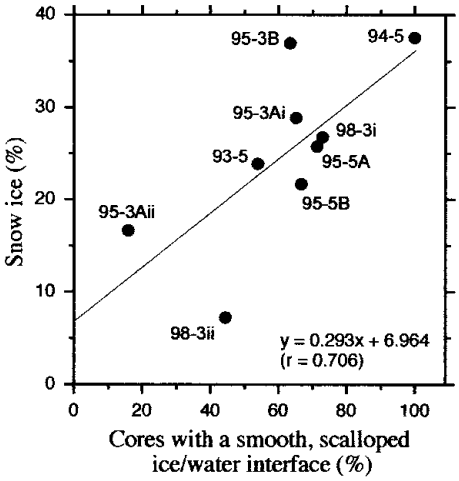

Fig. 6. Scatter plot of the amount of snow ice on each cruise as a function of the occurrence of bottom melting, as represented by the proportion of the total number of ice cores with a smooth, scalloped ice/water interface. The correlation coefficent (r) is statistically significant at the 95% confidence level.

NBP 94-5) regions had less congelation ice than the western region (164°E–150° W; NBP 95-3, 95-5A, 98-3);

2. there was less snow ice in the western region as a whole in 1998 than in 1995, but in both years there was strong zonation of the ice cover, with an outer pack ice dominated by snow ice and frazil ice (NBP 95-3Ai, 98-3i) and an inner pack ice dominated by congelation ice (NBP 95-3Aii, 98-3ii). The inner pack ice had much less snow ice in 1998 (NBP 98-3ii) than in 1995 (NBP 95-3Aii);
3. snow-ice formation was not temporally dependent, i.e. as much snow ice occurred in autumn as in winter.

The zonation of the Ross Sea according to the composition of the ice floes in autumn 1995 was reported by Jeffries and Adolphs (1997). That equally strong zonation should be observed 3 years later indicates that 1995 was not an anomalous year, and confirms that the Ross Sea is unlike other Antarctic sea-ice zones, including the central and eastern regions of this study, because of the large quantity of congelation ice that occurs there. In 1995, the boundary between the outer and inner pack ice, as defined by the contrasts in the amount of snow ice and congelation ice, was at 71° S, and in 1998 it was at 70° S (Fig. 5).

Jeffries and Adolphs (1997) attributed the differences in ice composition in the Ross Sea inner and outer pack ice to differences in environmental conditions. The outer pack ice is more stormy and dynamic, which favours frazil-ice and pancake-ice formation, and there is greater snowfall, which favours flooding and snow-ice formation. The inner pack ice has colder, calmer conditions, which favour congelation-ice growth, and a lower oceanic heat flux over the continental shelf, which reduces bottom melting. The greater snowfall on the outer pack ice is due to its proximity to a moisture source, i.e. the Pacific Ocean, from which there is a moist airflow. U.S. National Centers for Environmental Prediction re-analysis data for autumn 1998 show that periods of airflow from the Pacific Ocean were shorter and less frequent, and did not penetrate as far into the Ross embayment as they did in 1995 (K. Morris and others, unpublished data). Consequently, the snow cover on the Ross Sea pack ice was thinner and flooding of the snow/ice interface was less widespread in 1998 than in 1995 (Morris and Jeffries, 2001). Hence, in 1998, the amount of snow ice in the Ross Sea pack ice was smaller overall, and the snow-ice-dominated outer pack ice did not extend as far south as in 1995.

Apart from the Ross Sea inner pack ice over the continental shelf, the ice investigated in this study was on the deep ocean, where the oceanic heat flux would be expected to be higher than in shallower waters. McPhee and others (1996) have described the important role that the oceanic heat flux at the underside of the ice plays in determining the character of the ice cover through bottom melting. In this study, bottom melting, represented by the number of cores with a smooth, scalloped base and no skeletal layer, was common in autumn and winter, but was spatially and temporally variable (Fig. 6). It was least common in the inner Ross Sea in autumn (NBP 95-3Aii, 98-3ii), and most common in late winter in the outer Ross Sea pack ice (NBP 95-5A) and the central region (NBP 94-5). The amount of snow ice was moderately well correlated with the occurrence of bottom melting (Fig. 6). Bottom melting was much less widespread and there was a smaller amount of snow ice in the Ross Sea inner pack ice (NBP 95-3Aii, 98-3ii) than in the outer pack ice (NBP 95-3Ai, 95-3B, 95-5A) and the eastern region (NBP 93-5, 95-5B). The amount of snow ice was greatest in the central region (NBP 94-5), where the widespread bottom melting was attributed to the lateness of the season and a high oceanic heat flux (Jeffries and others, 1995, citing personal communications from H. H. Hellmer and S. S. Jacobs).

The effect of bottom melting has been likened to a conveyor belt (Ackley and others, 1995), where ice that melts off the bottom is replaced by snow ice at the snow/ice interface. Bottom melting, in effect, increases the snow load and the likelihood of flooding and snow-ice formation. It appears that high effective snow loads and the bottom-melting/snow-ice conveyor belt were particularly common in the Ross Sea outer pack ice, and the central and eastern regions of this study in autumn and winter.

If we consider only the bulk composition of the ice, it might be concluded that, in general, frazil-ice and/or congelation-ice formation dominated the development of the ice cover because one or the other, and sometimes both, exceeded the amount of snow ice (Fig. 5). However, the bulk composition gives a misleading impression of the importance of each ice type, as it does not account for the relative contributions of thermodynamic and dynamic thickening. Throughout the Antarctic sea-ice cover it has been found that ice cores are often composed of many layers of frazil and congelation ice (e.g. Eicken and others, 1991; Lange and Eicken, 1991; Worby and Massom, 1995; Jeffries and others, 1997, 1998). The individual layers of frazil and congelation ice represent the original, thermodynamically formed building-blocks of the ice cover, which subsequently thickened further by dynamic processes, i.e. rafting and ridging.

The relative importance of snow ice to the thermodynamic thickening of the ice cover can be judged by comparing the thickness of snow-ice layers to those of frazil ice and congelation ice (Fig. 7). We consider only the snow ice found as the uppermost layer of the ice cores, i.e. where it originally formed thermodynamically by the freezing of the mixture of snow and sea water/brine that resulted from flooding at the base of the snow cover. The few "buried" snow-ice layers that were observed have been excluded from the analysis as they are found below the surface as a result of dynamic processes (Lange and Hubberten, 1992; Worby and

https://doi.org/10.3189/172756401781818266 Published online by Cambridge University Press

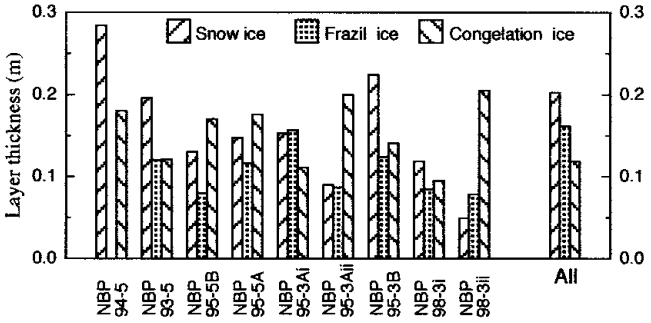

Fig. 7. Mean thickness of individual layers of snow ice, frazil ice and congelation ice in ice cores. Frazil-ice layer thickness data are not available for cruise NBP 94-5.

others, 1996). As Figure 7 shows, on five occasions the congelation-ice layers were thicker than the frazil-ice layers; on four occasions the snow-ice layers were thicker than the congelation-ice layers; and on six occasions the snow-ice layers were thicker than the frazil-ice layers. Snow ice and congelation ice, then, were often more important to the thermodynamic thickening of the ice cover than frazil-ice formation, and on some occasions snow ice was more important than congelation ice.

This is not to suggest that frazil-ice formation was unimportant in the development of the ice cover. On the contrary, here, as elsewhere in Antarctic waters, we believe that frazil ice played a vital role in the initial expansion of the pack ice through the "pancake cycle" in which rafting of the pancakes plays a large role in the dynamic thickening of the ice cover (Wadhams and others, 1987; Lange and others, 1989). However, once the initial frazil/pancake-dominated ice cover had formed and stabilized, snow ice and congelation ice were often more important to the subsequent thermodynamic thickening of the ice.

The importance of frazil ice to the thermodynamic thickening of the ice cover should not be underestimated, however. As Figure 7 shows, when the data from all five cruises are combined, the frazil-ice layers were thicker on average than the congelation-ice layers. But the data from all five cruises also show that, on average, snow ice made a greater contribution to the thermodynamic thickening of the ice cover than either frazil ice or congelation ice (Fig. 7).

Snow ice: a circum-Antarctic perspective

In the Weddell Sea, snow ice has been reported to make up as much as 16% of the ice volume (Lange and others, 1990; Lange and Eicken, 1991), and numerical simulations indicate that snow-ice formation is most likely to occur during the latter part of the ice-growth season (Eicken and others, 1995). In the East Antarctic pack ice, the amount of snow ice "is seasonally variable, with a lower percentage early in the growth season compared to spring" and has been reported as comprising 12–46% of the total ice volume during different cruises, and 13% for all cruises combined (Worby and others, 1998).

The pack ice in the Ross, Amundsen and Bellingshausen Seas is quite unlike that elsewhere, in that there is a greater amount of snow ice at any time of the winter compared to the Weddell Sea and East Antarctic pack ice. We attribute the greater amount of snow ice in the Ross, Amundsen and Bellingshausen Seas to greater snow loads and more extensive flooding. This is not because the ice is thinner than elsewhere. We have shown previously that in autumn and winter

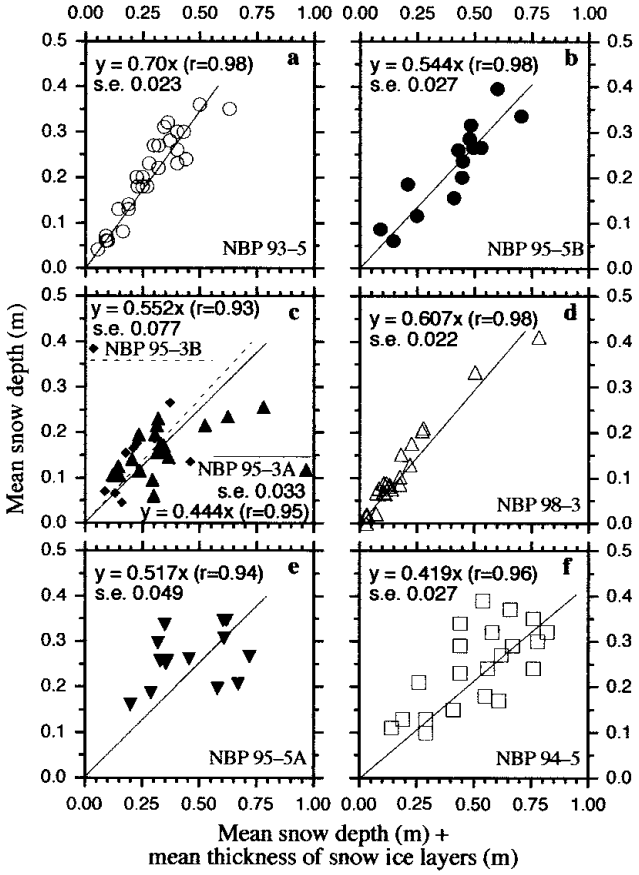

Fig. 8. Scatter plots of the mean snow depth as a function of the sum of the mean snow depth and the mean snow-ice layer thickness on each ice floe during each cruise. The correlation coefficents (r) for the regression equations/lines are statistically significant at the 95% confidence level. The standard error (s.e.) of the estimate of snow depth is given with each regression equation. The regression lines have been forced through the origin at zero on the assumption that, if there is no snow, neither flooding nor snow-ice formation will occur.

the ice in the Ross, Amundsen and Bellingshausen Seas is at least as thick as, and sometimes thicker than, in the Weddell Sea and the East Antarctic pack ice (Jeffries and Adolphs, 1997; Jeffries and others, 1998). Ship-based observations and remote sensing indicate that the snow depth on the ice in the Ross, Amundsen and Bellingshausen Seas is greater than elsewhere (Markus and Cavalieri, 1998). This, coupled with the fact that more snow ice forms in this region than elsewhere, indicates that there is greater snow accumulation and thus a greater snow load on the ice.

Snow-cover depletion and total snow accumulation

As the base of the snow cover floods and refreezes to form snow ice that contributes to the thermodynamic thickening of the ice cover, the depth of snow is reduced and the remaining snow does not represent the total amount of snow accumulation. This was illustrated with the NBP 94-5 and 95-3 data (Sturm and others, 1998) and predicted with a Weddell Sea ice model (Fritsen and others, 1998). In this subsection we estimate for each of the five cruises the proportion of the total snow accumulation that remained on the floes after snow-ice formation, and use that information to adjust the Set B snow-depth observations to derive estimates of the total snow accumulation on different ice-thickness categories.

To estimate the proportion of the total snow accumu-

https://doi.org/10.3189/172756401781818266 Published online by Cambridge University Press

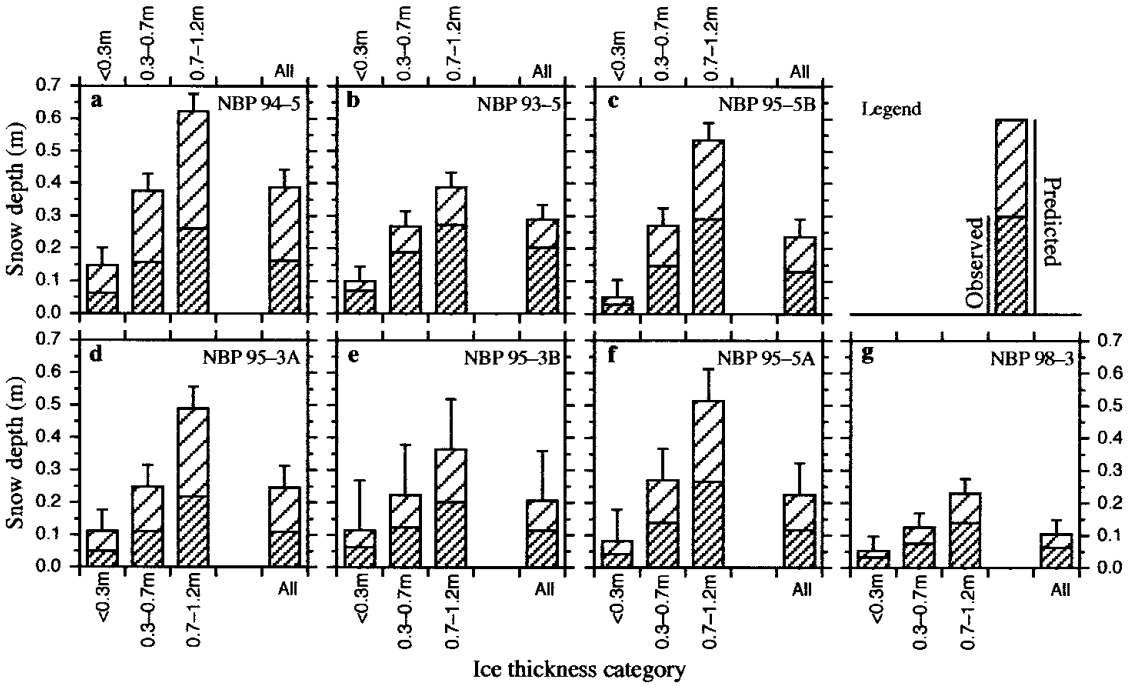

Fig. 9. Observed and predicted estimates of mean snow depth on three ice-thickness categories and on all categories combined during each cruise. The observed data, the Set B hourly snow-depth estimates, are represented by the short, closed cross-hatched bars. The predicted data, estimated using the regression equations in Figure 8, are represented by height of the open cross-hatched bars plus the closed cross-hatched bars below. The error bars are twice the standard error of the estimate of snow depth (see Fig. 8) and represent error estimates for the predicted snow-depth values at a 95% confidence level.

lation that remained on the floes, we assume that the thickness of the snow-ice layers is the same as the depth of snow lost to snow-ice formation. Then we regress the Set A mean snow depth against the sum of the Set A mean snow depth and the mean snow-ice layer thickness on each floe. The results (Fig. 8) show that there is some scatter in the data because: (1) we do not have as many snow-ice layers to average as we have Set A snow-depth measurements on each floe; (2) the Set A data include data from the tops of ridges, where the snow depth is reduced by wind erosion, and the flanks of ridges where snow depth increases due to deposition/drifting; (3) there might have been further snow accumulation since the last flooding and snow-ice formation event; (4) some fraction of snow might have been transferred off the floes into leads by the wind; and (5) there might have been some snow settling.

Despite the scatter, each regression line is statistically significant and the results indicate that as little as 42% of the total snow accumulation remained on the floes during cruise NBP 94-5 (Fig. 8f), while as much as 70% remained on the floes during cruise NBP 93-5 (Fig. 8a). When the data from all five cruises are combined, the regression equation, $y = 0.49x$ ($r = 0.95$), indicates that 49% of the total snow accumulation remained on the floes. The results of this analysis corroborate model predictions that flooding and snow-ice formation will reduce the snow depth by >50% (Fritsen and others, 1998).

The slopes of the regression lines offer the means to predict the total snow accumulation on the ice from the observed Set B snow-depth data. The results, presented in Figure 9, show the observed and predicted snow depth on three different Set B ice-thickness categories (<0.3 m, 0.3–0.7 m and 0.7–1.2 m) during each cruise. Ice >1.2 m thick has been excluded, as it includes an unknown amount of ridged ice, which is not part of this analysis of snow-ice formation and snow-cover depletion on the "level", unridged ice.

During each cruise, the observed and predicted snow depth increased as ice thickness increased (Fig. 9). This is to be expected, since thicker ice is generally older ice and has had more time to accumulate snow. That older ice accumulates more snow than younger ice is demonstrated by the ice in the central region, which was investigated in very late winter through very early spring and had the highest total snow accumulation of the entire study: a mean value of 0.38 m for all ice-thickness categories combined (Fig. 9a).

However, snow accumulation is not determined solely by the age of the ice. In autumn 1995 in the western region (Fig. 9d and e), the total snow accumulation was almost as great as it was in the eastern region in late winter 1993 and 1995 (Fig. 9b and c). The resultant early, high snow load would explain why there was as much snow ice in autumn in the western region, particularly in the outer pack ice, as there was in winter in the eastern region (Figs 3 and 5). The greater amount of precipitation on the younger ice cover in the western region may be due to regional and interannual differences in atmospheric circulation and moisture transport. As noted earlier, year-to-year differences in atmospheric circulation and moisture transport probably account for the lower observed and total snow accumulation in the western region in autumn 1998 (Fig. 9g) than in autumn 1995 (Fig. 9d and e), and the resultant differences in amount of snow ice, particularly in the inner pack ice (Figs 3 and 5).

SUMMARY AND CONCLUSION

Ice-core analysis shows that snow ice is common in autumn and winter throughout the first-year ice cover of the Ross,

https://doi.org/10.3189/172756401781818266 Published online by Cambridge University Press

Amundsen and Bellingshausen Seas. The snow that was entrained into the floes by flooding and snow-ice formation made a modest contribution to the total ice mass (3.6–7.3%), while the snow ice itself made a significant contribution to the total ice mass (12–37%) in all ice-thickness categories and even in autumn. Larger amounts of frazil ice and congelation ice were observed, but they owed their origin primarily to dynamic thickening. Snow ice, which forms primarily by freezing after the base of the snow cover has been flooded, often made a greater contribution to the thermodynamic thickening of the ice cover than either frazil ice or congelation ice. The important role that snow ice played in the thermodynamic thickening of the ice cover was enhanced by bottom melting that increased the effective snow loads and flooding at the base of the snow cover. Flooding and snow-ice formation depleted the snow cover and reduced its depth to 42–70% of the total snow accumulation depending on time and location. With this information it was demonstrated how ship-based snow-depth estimates could be adjusted to predict the total snow accumulation on different ice-thickness categories throughout the pack ice. Total snow accumulation was almost as great in autumn in the western region as it was in winter in the eastern region; hence the large amount of autumn snow ice in the western region. Adjusting ship-based estimates of snow depth to account for the depletion of the snow cover by snow-ice formation would make the growing body of in situ data more useful for the forcing and validation of numerical simulations of small- and large-scale sea-ice processes and atmosphere–ice–ocean interactions. Simulations must include flooding and snow-ice formation, and their accuracy will be judged by their ability to create significant amounts of autumn and winter snow ice such as those reported in this paper.

ACKNOWLEDGEMENTS

This research was supported by U.S. National Science Foundation (NSF) grants OPP-9117721, 9316767 and 9614844. We are grateful to the following who assisted with ice-core drilling and analysis: U. Adolphs, A. Belem, L. Chilton, S. Cushing-Shrout, C. Fritsen, M. Gowing, G. Hufford, R. Jaña, N. Kozlenko, E. Lawson, S. McCullars, K. Morris, M. Porter, T. Quakenbush, J. Sapiano, C. T. Sek, J. Stevens, T. Tin, J.-L. Tison, C. Venn, W. F. Weeks and A. P. Worby. We thank Captain J. Borkowski and the officers and crew of the R/V *Nathaniel B. Palmer*, and all Antarctic Support Associates personnel for their support aboard the ship and on the ice. B.H.-C. was supported in part by an NSF REU (Research Experience for Undergraduates) supplement. H.R.K. acknowledges the support of the Natural Sciences and Engineering Research Council of Canada for the Stable Isotope Laboratory, University of Calgary.

REFERENCES

Ackley, S. F., V. I. Lytle, G. A. Kuehn, K. M. Golden and M. N. Darling. 1995. Sea-ice measurements during ANZFLUX. *Antarct. J. U.S.*, **30**(5), Review 1995, 133–135.

Adolphs, U. 1998. Ice thickness variability, isostatic balance and potential for snow ice formation in ice floes in the south polar Pacific Ocean. *J. Geophys. Res.*, **103**(C11), 24,675–24,691.

Allison, I. 1982. The role of sea ice in climate variations. *In Report of the WMO/CAS-JSC-CCCO Meeting of Experts on the Role of Sea Ice in Climatic Variations, Geneva, 24–29 June 1982.* Geneva, World Meteorological Organization, 27–50. (World Climate Programme Report 26.)

Allison, I. and A. Worby. 1994. Seasonal changes of sea-ice characteristics off East Antarctica. *Ann. Glaciol.*, **20**, 195–201.

Drinkwater, M. R. and V. I. Lytle. 1997. ERS-1 radar and field-observed characteristics of autumn freeze-up in the Weddell Sea. *J. Geophys. Res.*, **102**(C6), 12,593–12,608.

Eicken, H., M. A. Lange and G. S. Dieckmann. 1991. Spatial variability of sea-ice properties in the northwestern Weddell Sea. *J. Geophys. Res.*, **96**(C6), 10,603–10,615.

Eicken, H., M. A. Lange, H.-W. Hubberten and P. Wadhams. 1994. Characteristics and distribution patterns of snow and meteoric ice in the Weddell Sea and their contribution to the mass balance of sea ice. *Annales Geophysicae*, **12**(1), 80–93.

Eicken, H., H. Fischer and P. Lemke. 1995. Effects of the snow cover on Antarctic sea ice and potential modulation of its response to climate change. *Ann. Glaciol.*, **21**, 369–376.

Fritsen, C. H., V. I. Lytle, S. F. Ackley and C.W. Sullivan. 1994. Autumn bloom of Antarctic pack-ice algae. *Science*, **266**(5186), 782–784.

Fritsen, C. H., S. F. Ackley, J. N. Kremer and C.W. Sullivan. 1998. Flood–freeze cycles and microalgal dynamics in Antarctic pack ice. *In* Lizotte, M. P. and K. R. Arrigo, *eds. Antarctic sea ice: biological processes, interactions and variability.* Washington, DC, American Geophysical Union, 1–21. (Antarctic Research Series 73.)

Jeffries, M. O. 1997. Describing the composition of sea-ice cores and the development of the Antarctic sea-ice cover. *Antarct. J. U.S.*, **32**(5), 55–56.

Jeffries, M. O. and U. Adolphs. 1997. Early winter snow and ice thickness distribution, ice structure and development of the western Ross Sea pack ice between the ice edge and the Ross Ice Shelf. *Antarct. Sci.*, **9**(2), 188–200.

Jeffries, M. O., R. A. Shaw, K. Morris, A. L. Veazey and H. R. Krouse. 1994a. Crystal structure, stable isotopes (δ^{18}O), and development of sea ice in the Ross, Amundsen, and Bellingshausen seas, Antarctica. *J. Geophys. Res.*, **99**(C1), 985–995.

Jeffries, M. O., K. Morris, A. P. Worby and W. F. Weeks. 1994b. Late winter characteristics of the seasonal snow cover on sea-ice floes in the Bellingshausen and Amundsen Seas. *Antarct. J. U.S.*, **29**(1), 9–10.

Jeffries, M. O., R. A. Jaña, S. Li and C. McCullars. 1995. Sea-ice and snow-thickness distributions in late winter 1993 and 1994 in the Ross, Amundsen and Bellingshausen Seas. *Antarct. J. U.S.*, **30**(1–4), 18–21.

Jeffries, M. O., A. P. Worby, K. Morris and W. F. Weeks. 1997. Seasonal variations in the properties and structural composition of sea ice and snow cover in the Bellingshausen and Amundsen Seas, Antarctica. *J. Glaciol.*, **43**(143), 138–151.

Jeffries, M. O., S. Li, R. A. Jaña, H. R. Krouse and B. Hurst-Cushing. 1998. Late winter first-year ice floe thickness variability, seawater flooding and snow ice formation in the Amundsen and Ross Seas. *In* Jeffries, M. O., *ed. Antarctic sea ice: physical processes, interactions and variability.* Washington, DC, American Geophysical Union, 69–87. (Antarctic Research Series 74.)

Lange, M. A. and H. Eicken. 1991. Textural characteristics of sea ice and the major mechanisms of ice growth in the Weddell Sea. *Ann. Glaciol.*, **15**, 210–215.

Lange, M. A. and H.-W. Hubberten. 1992. Isotopic composition of sea ice as a tool for understanding sea ice processes in the polar regions. *In* Maeno, N. and T. Hondoh, *eds. Proceedings of the International Symposium on the Physics and Chemistry of Ice, Sapporo, Japan.* Sapporo, Hokkaido University Press, 399–405.

Lange, M. A., S. F. Ackley, P. Wadhams, G. S. Dieckmann and H. Eicken. 1989. Development of sea ice in the Weddell Sea. *Ann. Glaciol.*, **12**, 92–96.

Lange, M. A., P. Schlosser, S. F. Ackley, P. Wadhams and G. S. Dieckmann. 1990. ^{18}O concentrations in sea ice of the Weddell Sea, Antarctica. *J. Glaciol.*, **36**(124), 315–323.

Lytle, V. I. and S. F. Ackley. 1996. Heat flux through sea ice in the western Weddell Sea: convective and conductive transfer processes. *J. Geophys. Res.*, **101**(C4), 8853–8868.

Lytle, V. I., K. C. Jezek, S. P. Gogineni and A. R. Hosseinmostafa. 1996. Field observations of microwave backscatter from Weddell Sea ice. *Int. J. Remote Sensing*, **17**(1), 167–180.

Maksym, T. and M. O. Jeffries. 2000. A one-dimensional percolation model of flooding and snow ice formation with particular reference to the Ross Sea, Antarctica. *J. Geophys. Res.*, **105**(C11), 26,313–26,331.

Maksym, T. and M. O. Jeffries. 2001. Phase and compositional evolution of the flooded layer during snow-ice formation on Antarctic sea ice. *Ann. Glaciol.*, **33** (see paper in this volume).

Markus, T. and D. J. Cavalieri. 1998. Snow depth distribution over sea ice in the Southern Ocean from satellite passive microwave data. *In* Jeffries, M. O., *ed. Antarctic sea ice: physical processes, interactions and variability.* Washington, DC, American Geophysical Union, 19–39. (Antarctic Research Series 74.)

Massom, R. A., M. R. Drinkwater and C. Haas. 1997. Winter snow cover on sea ice in the Weddell Sea. *J. Geophys. Res.*, **102**(C1), 1101–1117.

Massom, R. A., V. I. Lytle, A. P. Worby and I. Allison. 1998. Winter snow cover variability on East Antarctic sea ice. *J. Geophys. Res.*, **103**(C11), 24,837–24,855.

https://doi.org/10.3189/172756401781818266 Published online by Cambridge University Press

McPhee, M. G. *and 8 others*. 1996. The Antarctic Zone Flux Experiment. *Bull. Am. Meteorol. Soc.*, **77**(6), 1221–1232.

Morris, K. and M. O. Jeffries. 2001. Seasonal contrasts in snow-cover characteristics on Ross Sea ice floes. *Ann. Glaciol.*, **33** (see paper in this volume).

Morris, K., M. O. Jeffries and S. Li. 1998. Sea ice characteristics and seasonal variability of ERS-1 SAR backscatter in the Bellingshausen Sea. *In* Jeffries, M. O., *ed. Antarctic sea ice: physical processes, interactions and variability.* Washington, DC, American Geophysical Union, 213–242. (Antarctic Research Series 74.)

Rapley, M. and V. I. Lytle. 1998. Brine infiltration in the snow cover of sea ice in the eastern Weddell Sea, Antarctica. *Ann. Glaciol.*, **27**, 461–465.

Sturm, M., K. Morris and R. Massom. 1998. The winter snow cover of the West Antarctic pack ice: its spatial and temporal variability. *In* Jeffries, M. O., *ed. Antarctic sea ice: physical processes, interactions and variability.* Washington, DC, American Geophysical Union, 1–18. (Antarctic Research Series 74.)

Wadhams, P., M. A. Lange and S. F. Ackley. 1987. The ice thickness distribution across the Atlantic sector of the Antarctic Ocean in midwinter. *J. Geophys. Res.*, **92**(C13), 14,535–14,552.

Worby, A. P. and S. F. Ackley. 2000. Antarctic research yields circumpolar sea ice thickness data set. *EOS*, **81**(17), 181, 184–185.

Worby, A. P. and I. Allison. 1999. A technique for making ship-based observations of Antarctic sea ice thickness and characteristics. Part I. Observational techniques and results. *Antarctic CRC Res. Rep.* 14, 1–23.

Worby, A. P. and R. Massom. 1995. *The structure and properties of sea ice and snow cover in East Antarctic pack ice.* Hobart, University of Tasmania. Antarctic CRC. (Cooperative Research Centre Research Report 7.)

Worby, A. P., M. O. Jeffries, W. F. Weeks, R. Morris and R. Jaña. 1996. The thickness distribution of sea ice and snow cover during late winter in the Bellingshausen and Amundsen Seas, Antarctica. *J. Geophys. Res.*, **101**(C12), 28,441–28,455.

Worby, A. P., R. A. Massom, I. Allison, V. I. Lytle and P. Heil. 1998. East Antarctic sea ice: a review of its structure, properties and drift. *In* Jeffries, M. O., *ed. Antarctic sea ice: physical processes, interactions and variability.* Washington, DC, American Geophysical Union, 41–67. (Antarctic Research Series 74.)

World Meteorological Organization (WMO). 1970. *WMO sea-ice nomenclature: terminology, codes and illustrated glossary.* Geneva, Secretariat of the World Meteorological Organization. (WMO/OMM/BMO Report 259, TP 145.)

https://doi.org/10.3189/172756401781818266 Published online by Cambridge University Press